

Built-In Self-Testing Methodology and Infrastructure for an EMG Monitoring Sensor Module

Antonio José Salazar Escobar, José Machado da Silva,
Miguel Velhote Correia
INESC TEC e Faculdade de Engenharia,
Universidade do Porto,
Porto, Portugal
{†antonio.salazar,jms,mcorreia}@fe.up.pt

Bruno José Mendes
Unidade de Telecomunicações e Multimédia
INESC TEC (formerly INESC Porto),
Porto, Portugal
bruno.mendes@gmail.com

Abstract — Wearable technologies provide a refinement to personal monitoring by permitting a long-term on-person approach for capturing physiological signals. Sensors, textile integration, electronics miniaturization and other technological developments are directly responsible for advancements in this domain. However, in spite of the present progress, there are still a number of obstacles to overcome for truly achieving seamless wearable monitoring technology. That concerns, namely, improvements on the reliability of the system at the design stage, including the adoption of built-in self-test and embedded test instruments, features able to detect functional and structural failures. Biopotential monitoring has been part of medicine and rehabilitation protocols for decades now, thus its integration within wearable systems is a natural progression; nonetheless, a number of factors can affect acquisition reliability such as electrode-skin impedance fluctuations and the malfunction of the data-acquisition circuits. This article presents a built-in self-testing approach for an electromyography data acquisition unit, part of a wearable gait monitoring system. The approach makes use of the inter-integrated circuit bus in a dual purpose role, as a communication bus and for stimuli and test response propagation. The targeted tests are electrode-skin impedance checking through a straightforward threshold strategy and detection of functional deviations of the signal conditioning circuit of the electromyography unit, through a digital signature based approach.

Keywords - *BIST; EMG; electrode-skin impedance; digital signatures; structural faults; I2C.*

I. INTRODUCTION

The present paper provides an updated and extended description of the work presented by the authors at the GLOBAL HEALTH 2013 conference [1].

An increasing ageing population and consequently rising number of individuals with chronic movement and neurological disorders, are forcing societies to adapt to ever-growing demands. Currently, the capacity of most countries to address such alarming issue is inadequate, due to limited, understaffed and under-resourced facilities, proving ineffectual at times. For example, there were an estimated 10.3 million first-ever stroke survivors in 2005 worldwide [2] and stroke is projected to remain a leading cause of disability-adjusted life years (DALYs) [3] through 2030. Stroke care represents a major burden on global healthcare expenditures,

representing roughly 3% of healthcare costs [4]. Despite the cost, there exists a general agreement on the importance of addressing the sequelae of stroke. Concurrently, hip injuries and disorders are also likely to occur with aging. It is estimated that by the year 2030, the number of hip fractures in the USA will reach 289,000, an increase of 12% [5].

In order to safeguard the quality of life of the elderly and individuals with chronic ailments, a paradigm shift in the personal healthcare process is necessary; moving from a reactive (post-event) to a proactive (preventive) stand [6]. Nowadays, information and communication technologies (ICT) are supporting and promoting the aforementioned shift, by pushing health monitoring technologies closer to the end-user, in an effort to reduce costs through remote care. This way, the hospital based healthcare concept is being translated into smaller and more distributed health care services, including the home, up to the point where some health monitoring tasks can be done with the patient living her/his daily activities [7].

The use of portable devices for healthcare enables the early detection of abnormal conditions and facilitates the prescription of ambulatory treatments [8]. Until recently, most research involving the capture and analysis of biomedical and physiological signals has been limited to a laboratory or otherwise controlled environment, making use of cumbersome and costly equipment, which requires specialized facilities and trained personnel. Such practices, although useful in their own right, fail to consider real life scenarios and their impact on the subject. The fast paced developments of body sensor networks (BSN) and wearable technologies (including the so-called smart textiles) have allowed to open the next stage in human behaviour analysis tools, and introduce a new understanding of the interaction of individuals with their surrounding environment [9].

Although wearable and portable biomedical monitoring devices are rapidly becoming a recognized alternative, little attention has been paid to field testing protocols and methodologies, in order to insure measurement reliability, especially on long-term scenarios. When considering the reliability of wearable EMG monitoring systems, one can divide the focus in two main parts: that concerning the data

acquisition system and that dependent on the condition of the electrode-skin interface.

Testing and design for testability (DfT) have become a crucial aspect of most electronic designs; moreover, considering the structural complexities involved in modern packaging technologies. Intellectual property (IP) cores, hybrid technologies and mixed-signal systems have introduced a number of challenges that have dominated testing and development time and cost. Traditional approaches such as parametric characterization or hardware specific testing apparatus are far from providing the cost stabilizing effects achieved by automatic testing equipment (ATE) during the last decades of digital technology revolution. This is of particular concern when considering scenarios for remote or on-location monitoring solutions, which require constant self-diagnostic strategies in order to insure data reliability, such as the ones presented by wearable technologies. Additionally, the continuous tendency for mixed analog and digital (MAD) signal integration within modern designs drives towards new testing solutions, adapted to an evolving set of needs.

Although significant advances in the last decades have been made on the development and use of standard test infrastructures for digital circuits, such is not the case for analog or mixed-signal scenarios, in spite of the availability of the IEEE 1149.4 test bus [10] [11]. Nevertheless, a number of *ad hoc* contributions and strategies exist, where the general idea is the evaluation of an analog response to controlled stimuli, in order to verify expected response behaviors and correlating deviations to specific faults in certain cases [12] [13] [14].

In contrast, the electrode-skin interface [15] [16] [17], as well as its effect on biosignals measurements [18] [15] [16] [17] have been well studied. A number of studies and strategies exist on the electrode-skin impedance characterization domain [19] [20] [21], but the introduction of new electrode types (textile and capacitive for example) present novel challenges, especially in the case of electromyographic (EMG) signals acquisition [22]. The traditional approach for insuring quality electrode based bioelectric monitoring resorts to a thorough skin preparation of the target area, while qualified personnel positions the electrodes based on specific anatomical landmarks, verified with a portable skin-impedance meter or utilizing a test signal of the acquisition system. This approach is not readily applicable to certain subjects, such as elderly, allergenic and pediatric [23], or for most foreseen wearable strategies; moreover, variations of the electrode-skin interface impedance are to be expected [24]. Alternatively, methods such as those presented in [25] [26] provide a continuous monitoring of electrode-skin interface through the inclusion of additional hardware such as signal generators, current sources, and filters, used in parallel with the target signal acquisition components.

During biological signals capture, faults within modules (either catastrophic or parametric) can occur in both sensors

and signal conditioning circuitry. This is even more acute when these modules are integrated within wearable systems, due to the harsh conditions they are subjected to. The imprecise nature of electrical biosignals, combined with the parametric tolerance of the involved components; not to mention addressing transient variations caused by temperature changes, triboelectric and piezoelectric effects, positioning fluctuations, and sensor contact variation, require adopting testing approaches different from those used in traditional electronic scenarios. In order to improve the reliability of wearable systems, built-in testing and calibration functionalities are required for fault detection, localization and diagnosis prior data is erroneously captured.

This article presents a built-in self-testing (BIST) solution for an EMG sensor module of a wearable system intended for gait analysis. The strategy focuses on resource reutilization and component count minimization, through the reuse of an inter-integrated circuit (I²C) bus as a stimuli/response transport, managed through a novel protocol. Section II provides an overview of the wearable acquisition system for gait analysis on which the present work was based. Section III presents the implemented BIST strategies, as well as the management framework. Section IV summarizes the experimental test results, and Section V highlights the main conclusions and future developments of the work.

II. WEARABLE DATA ACQUISITION SYSTEM FOR GAIT ANALYSIS

Current instrumentation and methods for gait analysis are still expensive and complex, difficult to setup by healthcare staff, hard to operate and uncomfortable for the patient, while requiring a very high level of expertise for data gathering,

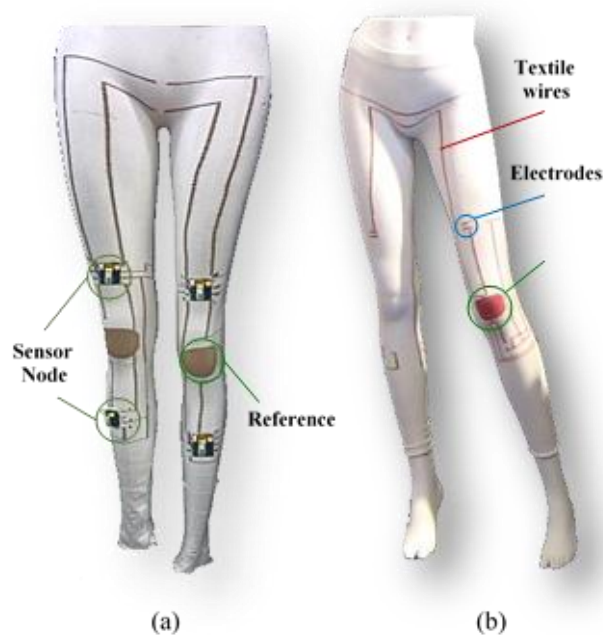


Figure 1. (a) Early prototype of gait analysis system. (b) Textile embedded wires and electrodes.

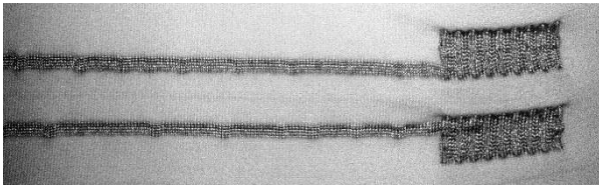


Figure 2. Embedded textile EMG electrodes.

analysis and interpretation. A new wearable instrument infrastructure specifically dedicated to capturing locomotion data is being developed [27]; an early prototype can be observed in Fig. 1 (a), while Fig. 1 (b) presents the textile embedding strategy that permits replacing cumbersome wiring; a close-up of the textile electrodes can be seen in Fig. 2.

This system includes, in a single infrastructure, the means to capture inertial and surface electromyographic signals (sEMG) of the lower limbs. It is presented as a network of sensor nodes interconnected through textile-conductive yarns and provides the measurement of kinematic variables, as well as the sEMG signals that are most important for locomotion. Each node comprises a sEMG sensor, an accelerometer, and a gyroscope, as well as an operation managing microcontroller responsible also for routing data in the established mesh network. EMG electrodes and the interconnections among sensor nodes are sewed on the leggings using yarns made with twisted filaments, each one a polymeric filament covered by a very thin layer of silver. Aggregated information is sent to a personal computer through a Bluetooth wireless link from a central processing module (CPM), as seen in Fig. 3.

The objective is to develop instrumented leggings for measuring human locomotion parameters in a practical and non-invasive way, even for people with strong impairments

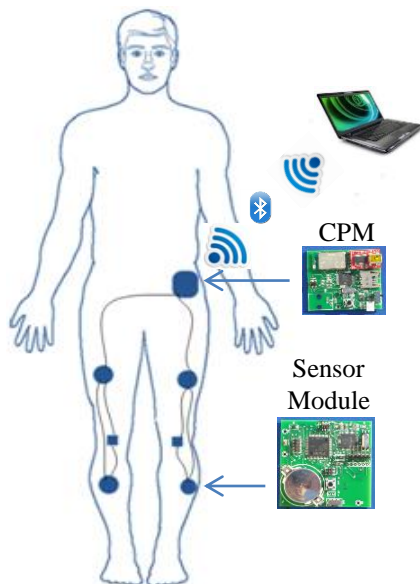


Figure 3. Gait analysis infrastructure.

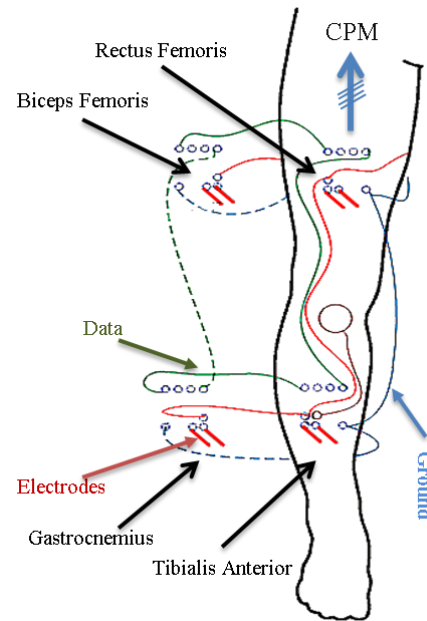


Figure 4. Gait analysis structure detailed view.

or disabilities. It is meant for capturing data, for prolonged periods of time, of typical movement activities under everyday living conditions, without interference or discomfort to the subject. The system allows the measurement of typical kinematic variables of the lower limbs, namely linear and angular movement of thighs and shanks, as well as the myoelectric signals of strategic muscles for locomotion analysis, as seen in Fig. 4, following recommendations from the Surface ElectroMyoGraphy for the Non-Invasive Assessment of Muscles (SENIAM) project [28] and a team of physiotherapists and specialists in gait analysis.

A. EMG Module

The EMG module contained within each sensor node, shown in Fig. 5, can be divided in two main sections: the electrodes and the signal conditioning circuitry (SCC). The electrodes are grouped in sets of two acquisition electrodes per targeted muscle plus a reference electrode per leg placed on the knee. The SCC comprises the following stages: an instrumentation amplifier, drift removal, filtering, gain adjustment, and a body reference drive feedback connected to the reference electrode. These stages have a predictable behavior established by their configuration and/or combination of elements such as resistors and capacitors, which show an acceptable dispersion of values among them, maintaining the proper functioning of the system. However, variations in the manufacturing process of the components, different life-time degradations, electrical faults (shorts and open circuits), or environmental issues such as, humidity, pressure or temperature, can alter such balance of values.

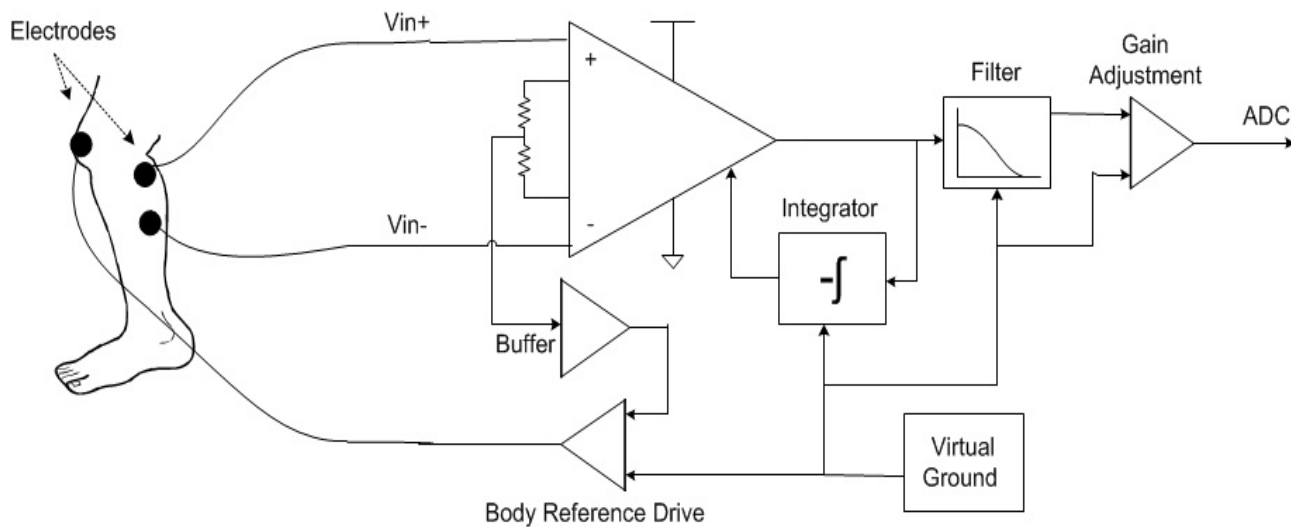


Figure 5. EMG signal conditioning module structure.

Therefore, it is important to ensure that the system is operating within the defined limits before and during its usage, in order to insure the reliability of the captured data.

III. BUILT-IN SELF-TESTING

Built-in self-testing/calibration (BISTC) strategies have traditionally focused on performing detection, diagnosis and repair actions of a specific module, section, component, or IP core [29] [30]. The increasing complexity of modern wearable monitoring technology (WMT) can seldom benefit from strategies that are either too centralized, external data/equipment dependent, or component focused. Communication and area overhead, increased complexity and resources, or energy expenditure, are just a few factors that limit traditional approaches.

In order to address some of the aforementioned limitations, a BIST structure was proposed, which reduces

implementation overhead, in terms of design time, pin-count and board area, through the reuse of the I2C bus (already used for connecting the accelerometer and the gyroscope) for testing management purposes, as seen in Fig. 6. Such approach permits taking advantage of the I2C bus, generally present within wearable systems for multi-component communication, as a means for stimuli/response transport, as well as for testing management. Further explanation of the methodology can be found in Section IIIC.

In this particular scenario the embedded instrument refers to the EMG module previously described. The approach seeks to integrate within the module elements required for testing different aspects, such as the electrode-skin impedance for proper sensor contact verification, as well as the signal conditioning circuitry functional response. In such setup, a switching matrix that manages the different signals

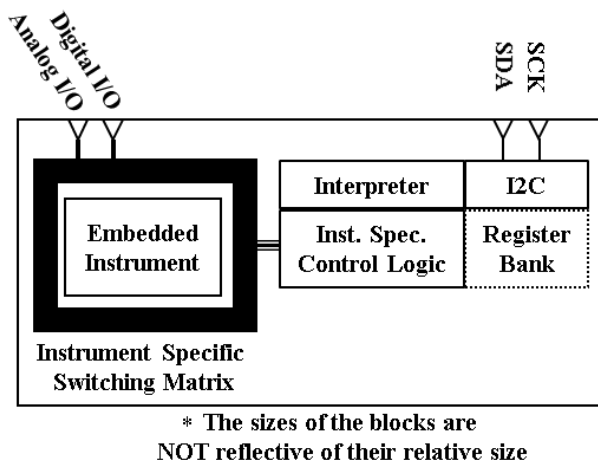


Figure 6. Overview of generic embedded instrument with proposed infrastructure.

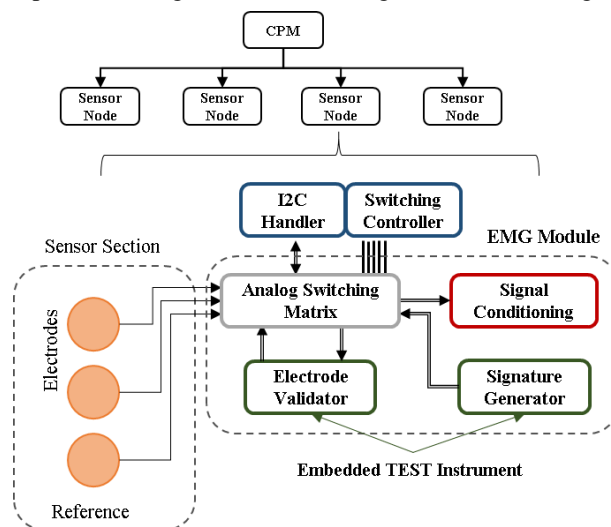


Figure 7. EMG module BIST structure.

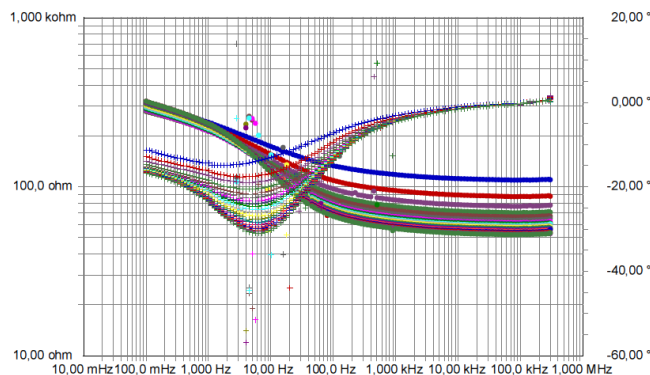


Figure 8. Electrode-Gel time lapse impedance.

routing is necessary to perform the necessary actions, with special consideration to active operation time synchronization, i.e., meaning that safety considerations are also in play due to the nature of the electrode-skin interface. Fig. 7 presents an overview of the strategy applicable to the described scenario, where the signature generator and electrode validator stand for the circuitry utilized for testing; which will be described in the next sections.

A. Electrode-skin Verification

Surface electrodes are likely the most utilized sensors for capturing electrical biosignals measurements, such as electrocardiography, electromyography, electroencephalography, electrooculography, bioimpedance, impedance tomography, among others. The contact impedance achieved in the electrode-skin interface affects biosignals measurements (as stated earlier), a matter of concern, traditionally solved through, namely, skin preparation procedures, equipment checking, and electrode replacement. Even under such controlled conditions, variations of the electrode-skin contact impedance are to be expected. However, in applications such as daily activities monitoring and the performance measurement of an athlete, or other scenarios where the individuals will have to position the electrodes themselves or the electrodes are integrated within a garment, careful positioning and skin preparation cannot be guaranteed.

Fig. 8 presents an eight hour time lapse measurement of the impedance of a commercially available disposable pediatric Ag/AgCl foam electrodes, of 1 cm of diameter core and 3 cm of diameter foam (DORMO, ref SX-30) over an Agar based gel, following the preparation procedures presented in [31]. A conventional three electrode setup with a GAMRY Series G-300 Galvanostat with 50 μ A stimuli compatible with IEC 60601-1 standard [32] and ANSI/AAMI EC12:2000 recommendations [33], was performed in a controlled environment in order to ascertain the time variation of the electrode material interface impedance. As can be observed in Fig. 8, there is a prolonged settling period caused mainly by hydrophilic effects and temperature equilibration between the two interacting elements, similar to

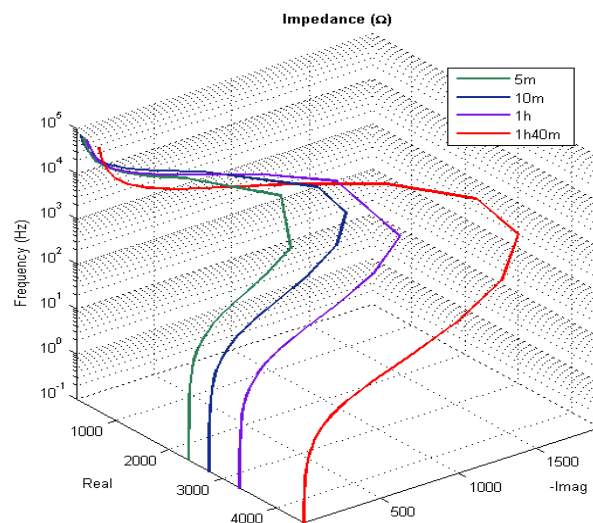


Figure 9. Time lapsed electrode-skin impedance.

the effect reported on the electrode-skin interface [34], observed in Fig. 9 as well.

Fig. 9 presents the measurements of an electrode-skin interface of a human volunteer. The skin was prepared with a straightforward technique, limited to light shaving, degreased with alcohol, dead cells removed with a soft brush, later cleansed with soap and water, and allowed to rest for 10 minutes. The target electrode and its reference were located roughly 3 cm proximal to the elbow and the signal injection electrode roughly 6 cm from the center point of the target-reference electrode line, proximal to the forearm mid-point (all measurements were considered from the center of the electrodes), the ground electrode was located at the contralateral posterior side elbow, as seen in Fig. 10. The subject was then placed within a Faraday cage, in order to reduce electromagnetic noise, following a sitting position with the forearm containing the electrodes resting

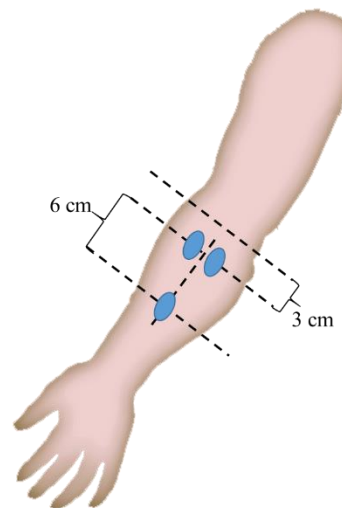


Figure 10. Electrode placement.

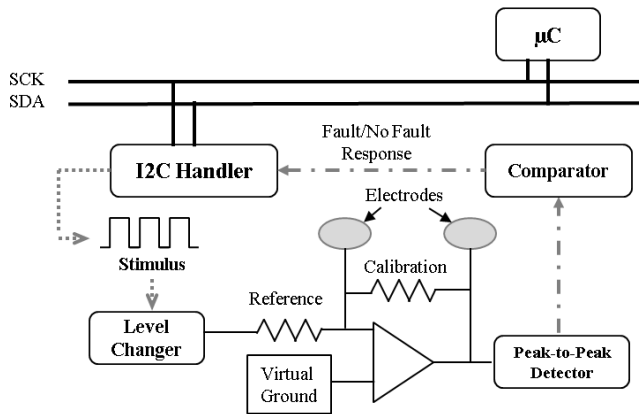


Figure 11. Electrode-skin verification structure.

horizontally. As can be observed in Fig. 9, a similar hydrophilic phenomenon occurred as in the case of the electrode-gel. Such phenomenon is known by healthcare personnel, reason for which most electrode related procedures include a settling period prior to measurements.

The phenomenon described above is worth mentioning in order to illustrate the variability of the electrode-skin interface; although it is not the greatest concern within a wearable system. Conventionally, analog faults are classified as hard (catastrophic) or soft (parametric), referring to the trace continuity; however, when considering sensors, the fault classes are not so well defined. For instance from a data centric point of view one can summarize, following [35] [36] [37] [38] [39]:

- *Constant* or dead: measures provide invariant arbitrary values, uncorrelated to the observed phenomenon.
- *Random noise*: increased variance of the target sensor measurements.
- *Short*: sharp momentary irregularities between measurement points.
- *Accumulative or drift*: continuous deviation trend from the correct value, expressible through a deterministic relation with true value, possibly cause by age, decay, damage, etc.

In the case of textile electrodes the problems are exacerbated, due to their sensitivity to pressure, fabric stretching, and motion artifacts [40] [41] [42]. In addition, textile electrodes and wires, such as those presented back in Fig. 2, are relatively new technologies and strong behavioral models have not been well established when compared to pre-gel electrodes; which complicates issues related to interface impedance variability.

Several approaches have been implemented, through the years, for the measurement and monitoring of the electrode-skin impedance, such as the ones presented in [18] [20] [21] [25] [26] [34]. An electrode-skin impedance verification circuit was developed following a straightforward approach, based on the injection of a low amplitude stimulus current (less than $10\mu\text{A}$) in order to ascertain an electrode pair target load. Individual electrode-skin interface strategies generally utilize a three electrodes approach (one electrode-skin contact

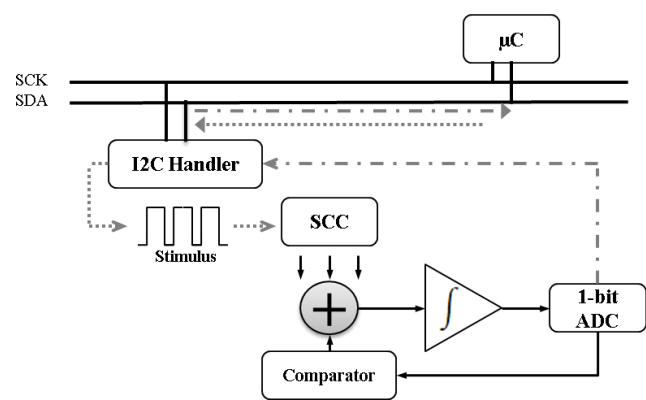


Figure 12. SCC test infrastructure.

target and two others for sinking and voltage reference respectively).

However, an electrode pair-wise verification was preferred in this case, in order to maintain simplicity. A single-supply current to voltage converter was used as observed in Fig. 11, which includes a calibration resistor in parallel with the target load in order to control threshold limits and avoid open feedback scenarios. The configuration follows that of a current controlled voltage source, where the current observed across the reference resistor flows towards the electrodes and calibration resistance generating a voltage proportional to the impedance under test. Momentary sharp irregularities are limited by the calibration resistor, as well as stabilizing capacitors (not observed in the figure). The magnitude of the stimulus current is a paramount consideration due to the possible negative effects in the human body, hereby achieved through the introduction of a limiting reference resistor. A local DC reference can be applied as stimulus in addition to a virtual ground compensated square wave signal sent through the I2C bus.

B. Signal conditioning circuitry verification

Common-mode rejection, amplification and filtering are regular stages of any electrode based signal conditioning circuit [42][48]. These are required to reduce the effects of common-mode potentials, random noise, motion and power-line artifacts, as well as to effectively retrieving the components of interest of the measured signal. Amplification factors and cut-off frequencies are dependent on the signal type [42][48], and deviations can cause unwanted elements to be introduced into the captured signal.

The test of the SCC (see Fig. 12) is achieved by means of the injection of an impulse stimulus at the input, fusion of the response of targeted nodes within the SCC, and the collection of the final response in the form of a digital signature that can be compared against a response table, composed by a set of signatures corresponding to the tolerance determined by acceptable components variations.

Initially, a Built-In Logic Block Observer (BILBO)-like [43] based approach was attempted in which the stimulus was

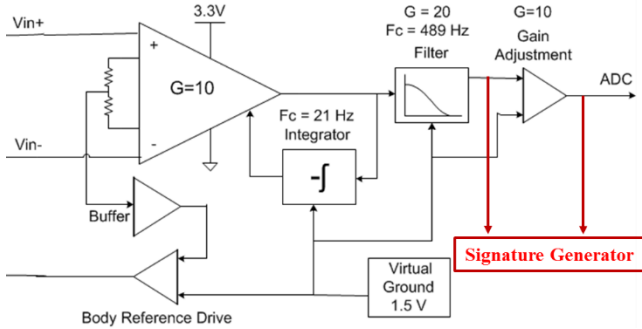


Figure 13. SCC target test nodes.

provided by an LFSR (Linear Feedback Shift Register), and the response of the SCC was collected by a Multiple Input Signature Register (MISR). These are solutions commonly found in the structural test of digital circuits, which are prone to aliasing errors, i.e., there is a (small) probability that the signature of a bad circuit is the same as that of a good circuit. In fact, such solution proved to be ineffective in the present case, since large variations of some components of the SCC module rendered signatures not so different from those obtained considering valid values, thus providing unreliable and ambiguous error detecting methods for this specific purpose.

Alternatively, a different testing approach was chosen, where a delta-sigma ($\Delta\Sigma$; or sigma-delta, $\Sigma\Delta$) like modulator is used to convert the SCC response into a bit stream, being the I2C bus used for stimulus generation and response capture purposes (Fig. 12). An I2C bus driven stimulus was preferred over a locally generated one, in order to reduce local sources of noise (such as clocks), gain increased stimulus shaped flexibility, and reuse of existing resources. The target observation nodes were determined through a sensitivity analysis after a SPICE simulation, which established that the low-pass filter output and the ADC input are the nodes that best reflect variations within the components of the SCC, seen in Fig. 13.

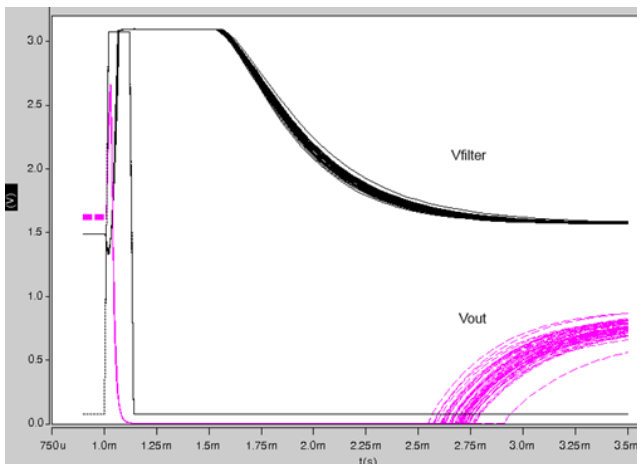


Figure 14. SCC response to the test stimulus.

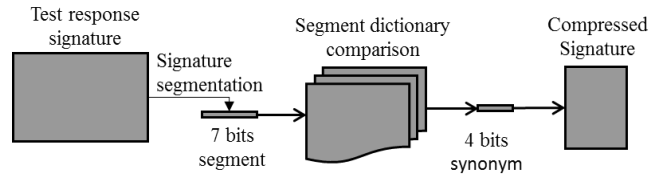


Figure 15. Compression algorithm overview.

The SCC test impulse is designed to stimulate the SCC frequency bandwidth and amplitude full range. The observation of different analog nodes and their compression into a single bit stream improves observability and saves test response resources and time. This way, the need for an analog test bus line, the inclusion of a bulky analog to digital converter, and the need for a multiplexed test response acquisition are avoided. Fig. 14 shows the test impulse response, of the two selected inputs to the signature generator for a Monte Carlo simulation considering 10% variations of the SCC's capacitors and resistors values.

In order to reduce noise along the communication lines, complexity and total area of the test circuit, it was decided to differ from traditional $\Delta\Sigma$ modulators, by eliminating the flip-flops generally present between comparators. The output of the signature generator is kept in a non-ground state through the use of a pull-up resistor until the test stimulus forces the first '0', to ensure a known initial condition and thus a predictable start sequence, compatible with I2C as well. After such start event, the signal is captured every 10 μ s during 1.05 ms generating a 105-bit long signature.

The resulting signature is acquired through the I2C bus by the local processing module, which applies a window bit density filtering and Ziv-Lempel based lossless compression algorithm [44]. As the SCC test response presents variations due to the acceptable tolerances of its components, the golden signature is actually a set comprising the signatures of different admissible responses.

The Ziv-Lempel based lossless compression algorithm replaces repetitive bit sequences by a shorter code, as described in the following pseudo-code and observed in Fig. 16:

```

array =  $\Delta\Sigma$  output
foreach segment from array
  if segment  $\in$  dictionary
    then signature += segment
foreach segment from signature
  if segment  $\in$  2nd dictionary
    then final signature += segment
    
```

Figure 16. Pseudo-code for compression algorithm.

The use of this compression algorithm is twofold. On one hand, compression allows reducing the length of data to be transmitted along the wired network from the sensor node to the CPM, as well as through the Bluetooth link, thus reducing communication time and power. On the other hand, it allows to recover the original analog response at an external

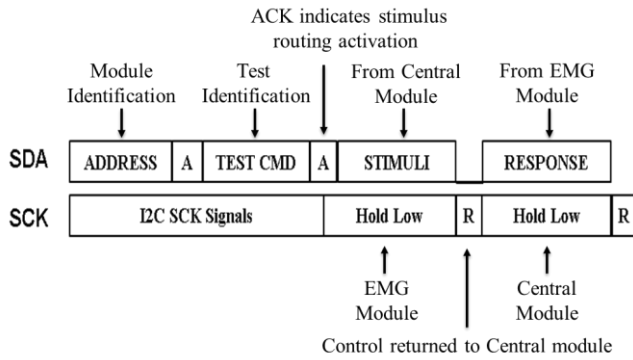


Figure 17. I2C compatible sequence for Stimulus/Response transport.

processing unit, using a corresponding decompressing algorithm.

C. I2C bus and test management handler

A testing and/or calibration strategy for WMT benefits from distributed or multi-sensor aware approaches. Such approach could seek to maintain data reliability after the recognition of deviating degradation patterns on sensors that could provide insight into system problems due to, e.g., improper sensor positioning, induced electrical effects due to movement (turboelectric and piezoelectric effects), structural flaws and other factors that require the coverage provided by the analysis of multiple temporal instances, redundant structures comparison, or introspection into fused data components. In order to manage the previously mentioned approach, a testing framework was designed based on a protocol named SCPS [45]; which seeks to standardize the command sequence for sensor acquisition/testing access.

In the present case, an instruction enables a testing procedure, activating pre-determined routing configurations. It is possible as well to use an I2C compatible sequence for transporting stimuli and responses to and from the target module as described in Fig. 17.

The sequence sets up the appropriate routing configuration through acknowledgement of a test command and uses the next two SCK low-state for stimulus and response transport. In order to avoid start/stop events from occurring, the master element insures a low-state of the SDA prior to SCK high. A re-start or stop event can then be used at the event of the sequence to finalize the action.

IV. RESULTS

The electrode verification circuit was first simulated on Multisim 11.0.775, for functional and electrical parameters validation and to confirm the suitability of the arrangement. Preliminary experiments were then performed on an Agar based gel for performance verification prior to testing on human volunteers. A number of signals were used for behavioral confirmation, as can be seen in Figs. 18, 19, and 20.

The electrode-skin impedance was changed through variations of the contact surface between the electrode and

the skin, Fig. 18 presents different responses of the circuit to such variations for a 10 μ A DC stimulus, demonstrating its sensitivity to the electrode-skin impedance variations, thus compatible with a threshold based fault detection approach. Fig. 19 and Fig. 20 present corresponding responses to square-wave and sine-wave, respectively, stimuli of matching peak to peak amplitude, respectively (limited to 50 μ A). These responses also demonstrate their sensitivity to the reactive component of the electrode-skin impedance (through phase and time response effects), by presenting a measurable

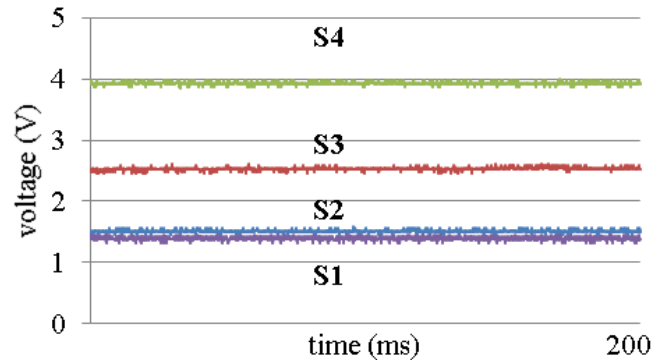


Figure18. DC Stimuli response for varying conditions, where S1 is the stimuli, S2 is low impedance response, S3 is an expected impedance response and S4 is a high impedance response.

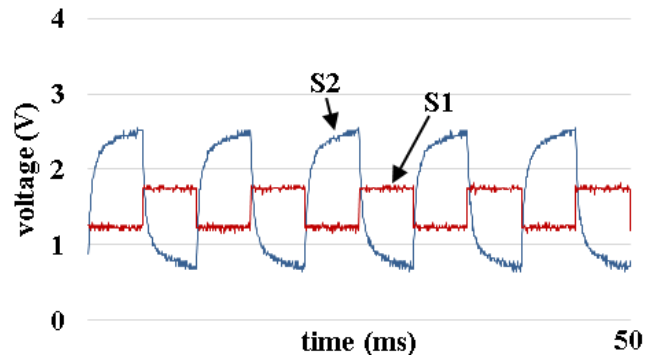


Figure 19. Square wave of 100 Hz stimuli, where S1 is the stimuli, and S2 is an expected impedance response.

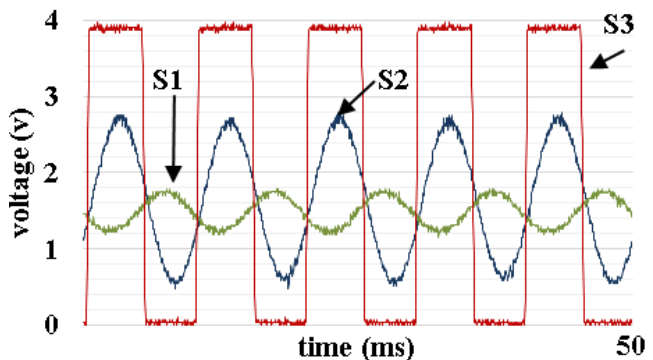


Figure 20. Sine wave of 100 Hz stimuli response for varying conditions, where S1 is the stimuli, S2 is a normal impedance response and S3 is a high impedance response.

phase difference in the case of S2 within Fig. 19 and through the behavior of S2 in Fig. 20, showing a classical charging/discharging behavior. On the other hand, the S3 saturation level seen in Fig. 19 corresponds to an unacceptable over the limit electrode-skin impedance case.

A. Signature generation results

The SCC and the $\Delta\Sigma$ circuits were simulated within a SPICE like simulator, using the models of manufacturers for the operational amplifiers, comparators and analog switches. Figs. 21 to 24 show the waveforms obtained in response to the test impulse, for golden and faulty cases. The input pulse stimulus was designed considering the circuit time constants and the I2C time specifications – I2C's fast-mode and fast-mode plus specifications impose minimum durations of 0.6 μs and 0.26 μs high periods, respectively [46].

Figs. 22, 23, and 24 present faulty responses for the cases of, respectively, a 5% reduction of the filter gain, a 30% reduction of the low-pass filter capacitor value, and an open connection in the instrumentation amplifier – Fig. 21 shows the golden response. The sequences of pulses presented in each case are the corresponding outputs of the $\Delta\Sigma$ modulator. It can be seen that, after comparing these sequences with the golden case, the three faults are detectable as different bit streams are generated.

The direct capture of these test responses is possible because the I2C sampling frequency allows doing it with an adequate resolution, i.e., no pulses are lost.

Experimental results were obtained with a demonstration prototype. For that purpose faults were introduced in the SCC in some of the most critical components for the proper operation of the circuit. According to the literature, the low-pass filter cutoff frequency (f_c) for EMG signal conditioning

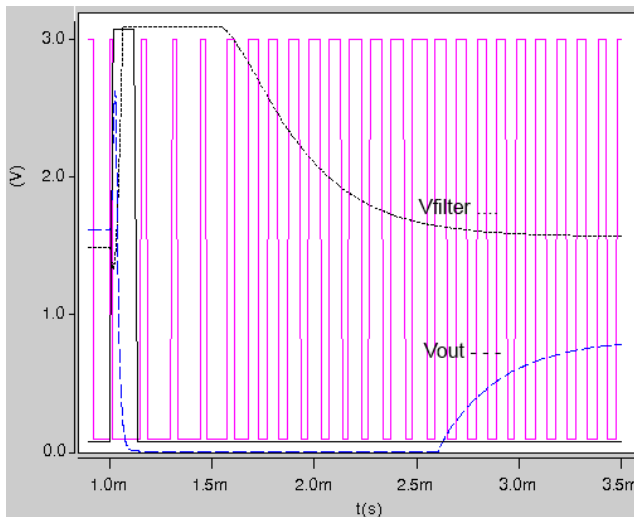


Figure 21. Signature generator input signals (Vfilter; Vout) and $\Delta\Sigma$ output – golden case.

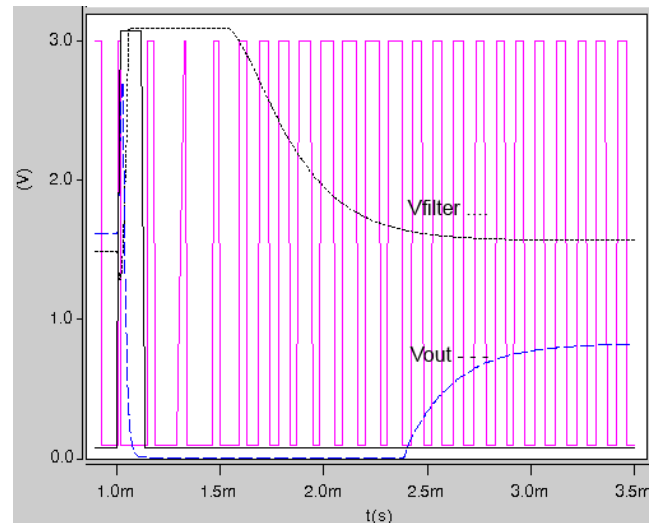


Figure 23. Signature generator input signals (Vfilter; Vout) and $\Delta\Sigma$ output – 30% reduction of a capacitor value.

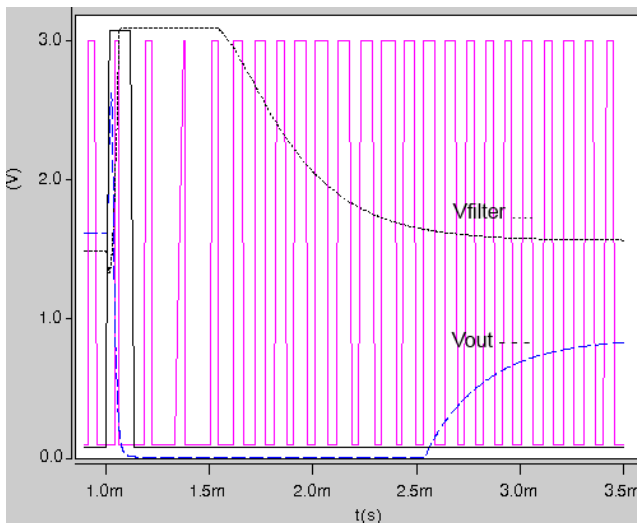


Figure 22. Signature generator input signals (Vfilter; Vout) and $\Delta\Sigma$ output – 5% reduction of the filter gain.

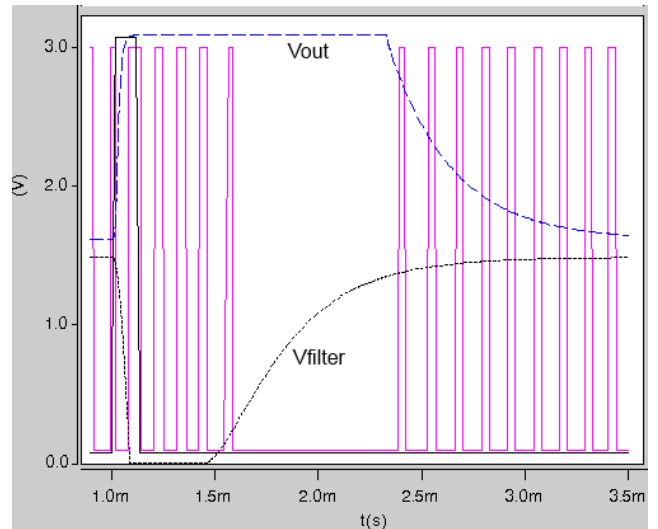


Figure 24. Signature generator input signals (Vfilter; Vout) and $\Delta\Sigma$ output – open circuit in the instrumentation amplifier.

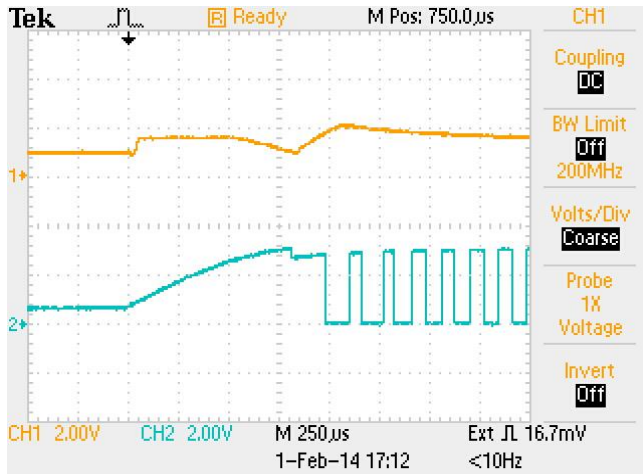


Figure 25. Cutoff frequency at 482 Hz.

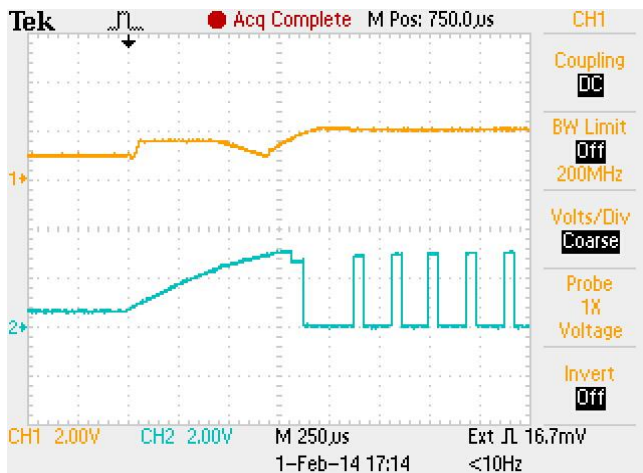


Figure 26. Cutoff frequency at 1.45 kHz.

circuits should be considered in the range from 500 Hz [28] to 700 Hz [47] or even 1000 Hz [48]. In our case, the tolerance band of the cut-off frequency imposed by the admissible components variations, shows a width from 480 Hz to 800 Hz. Deviations were introduced in some components in order to change the cutoff frequency to values inside and out of the tolerance band, i.e., $f_c = [300, 492, 688 \text{ Hz}, 1450, 10130] \text{ Hz}$.

In Figs. 25 and 26 one can see the input (yellow/top signal) and the output (blue/bottom signal) of the test signature generator in case of, respectively, an acceptable and an unacceptable cutoff frequency. The bit-stream that is then obtained presents a duration of 1.05 ms, or a length of 105 bits.

After compressing, the captured bit-streams are compared against the expected golden responses. This is achieved by evaluating the bits in specific windows, where common patterns are produced among good responses. Fig. 27 shows the compressed signatures obtained for valid (top three) and faulty (bottom four) responses, corresponding to deviations of the cutoff frequency to $f_c = [300, 1450, 2500, 10130]$. A



Figure 27. Valid (top three) and faulty (bottom four) test signatures.

circuit is considered faulty when the bits in the evaluation windows are different from the expected ones.

V. CONCLUSION AND FUTURE WORK

A significant research effort has been made to develop economic and reliable tools capable of providing, as non-obtrusive as possible, portable monitoring of biological signals. Many of the solutions that have been proposed so far are based on placing sensors on garments that can be worn without any extra special care. However, the testing of these electronic systems has not deserved the same attention and solutions are required in order to improve that reliable data is captured and used in medical protocols.

The inclusion of testing features within wearable technologies is of paramount importance due to their portable nature and target monitoring scenarios. In contrast with medical devices found within hospital and healthcare facilities, wearable healthcare systems do not necessarily count with the support of professional personnel to verify their placement and continuous operation.

A mixed-signal built-in self-test infrastructure and methodology is presented that addresses the in-situ verification of the electrode-skin interface, as well as the functionality of the signal conditioning circuitry of a wearable electromyographic data acquisition system. The approach being proposed uses an I2C bus for test event management and stimuli/response transport, through a protocol meant for resource optimization and sensor group testing strategies. The electrode-skin interface is evaluated after the measurement of the complex impedance and the signal conditioning circuitry is tested after comparing its impulse response with the expected golden response. A Ziv-Lempel compression algorithm is used to allow transferring a shorter version of the captured bit stream, thus saving communication time and power, while preserving the possibility of reconstructing the impulse response of the circuit. The simulations and circuit implementation results confirm the validity of the approaches being proposed and reveal their compatibility to the target system and available resources.

This work is expected to be further developed with the design of new versions of the proposed test instruments, namely with the on-chip implementations, and the design of instruments to test other parts of the systems, always using the SCPS infrastructure for test data and operations management.

ACKNOWLEDGMENT

This work was financed by the ERDF – European Regional Development Fund through the COMPETE Programme (operational programme for competitiveness) and by National Funds through the *Fundação para a Ciência e a Tecnologia* (Portuguese Foundation for Science and Technology) within project ProLimb PTDC/EEA-ELC/103683/2008, grant SFRH/BD/61396/2009, and project ELESIS/ENIAC - European Library-based flow of Embedded Silicon test Instruments.

REFERENCES

- [1] A. Salazar, B. Mendes, J. Da Silva, and M. Correia, "Built-in self-testing infrastructure and methodology for an EMG signal capture module," Proc. 2nd International Conference on Global Health Challenges (GLOBAL HEALTH 2013), Lisbon, Portugal, 2013, pp. 43-48.
- [2] K. Strong, C. Mathers, and R. Bonita, "Preventing stroke: saving lives around the world," *Lancet Neurol.*, vol. 6, no. 2, 2007, pp. 182-187.
- [3] A. D. Lopez, C. D. Mathers, M. Ezzati, D. T. Jamison, and C. Murray, "Global and regional burden of disease and risk factors, 2001: systematic analysis of population health data," *The Lancet*, vol. 367, no. 9524, May 2006, pp. 1747 – 1757.
- [4] S. M. Evers, J. N. Struijs, A. J. Ament, M. L. van Genugten, J. H. Jager, and G. A. van den Bos, "International comparison of stroke cost studies," *Stroke*, vol. 35, no. 5, April 2004, pp. 1209-1215, doi: 10.1161/01.STR.0000125860.48180.48.
- [5] J. A. Stevens and R. A. Rudd, "The impact of decreasing U.S. hip fracture rates on future hip fracture estimates," *Osteoporosis International*, vol. 24, no. 10, Oct. 2013, pp. 2725-2728, doi:10.1007/s00198-013-2375-9.
- [6] J. Yoo and H. Yoo, "Emerging low energy wearable body sensor networks using patch sensors for continuous healthcare applications," Proc. of the Int. Conf. IEEE Engineering in Medicine and Biology Society (EMBC), Aug.-Sept. 2010, pp. 6381-6384, doi: 10.1109/IEMBS.2010.5627299.
- [7] M. Engin, A. Demirel, E. Z. Engina, and M. Fedakarc, "Recent developments and trends in biomedical sensors," *Measurement*, vol. 37, no. 2, March 2005, pp. 173-188, doi: 10.1016/j.measurement.2004.11.002.
- [8] A. Pantelopoulus and N. G. Bourbakis, "A survey on wearable sensor-based systems for health monitoring and prognosis," *IEEE Transactions on Systems, Man, and Cybernetics*, vol. 40, no. 1, Jan. 2010, pp. 1-12, doi: 10.1109/TSMCC.2009.2032660.
- [9] M. Chen, S. Gonzalez, A. Vasilakos, H. Cao, and V. C. Leung, "Body area networks: a survey," *Mobile Networks and Applications*, vol. 19, no. 2, April 2011, pp. 171-193, doi:10.1007/s11036-010-0260-8.
- [10] L. T. Wang, C. W. Wu, and X. Wen, *VLSI test principles and architectures: design for testability*, Academic Press, 2006.
- [11] "IEEE 1149.4 Mixed-Signal Test bus Working group," [Online]. Available: <http://grouper.ieee.org/groups/1149/4>. [Accessed May 2014].
- [12] L. S. Milor, "A tutorial introduction to research on analog and mixed-signal circuit testing," *IEEE Trans. on Circuits and Syst.*, vol. 45, no. 10, Oct. 1998, pp. 1389-1407, doi: 10.1109/82.728852.
- [13] B. Kaminska and K. Arabi, "Mixed signal DFT: a concise overview," Proc. Int. Conf. on Computer Aided Design, San Jose, Nov. 2003, pp. 672-679, doi:10.1109/ICCAD.2003.1257882.
- [14] S. R. Das, J. Zakizadeh, S. Biswas, M. H. Assaf, A. R. Nayak, E. M. Petriu, W. Jone, and M. Sahinoglu, "Testing analog and mixed-signal circuits with built-in hardware: a new approach," *IEEE Trans. on Instr. and Measurement*, vol. 56, no. 3, June 2007, pp. 840-855, doi:10.1109/TIM.2007.894223.
- [15] J. J. Huang and K. S. Cheng, "The effect of electrode-skin interface model in electrical impedance imaging," in Proc. Int. Conf. on Image Processing, vol. 3, Oct. 1998, pp. 837-840, doi:10.1109/ICIP.1998.727384.
- [16] D. J. Hewson, J. Druchêne, and J. Y. Hogrel, "Changes in impedance at the electrode-skin interface of surface EMG electrodes during long-term EMG recordings," in Proc. 23rd IEEE EMBS, vol. 4, Oct. 2001, pp. 3345-3348, doi: 10.1109/IEMBS.2001.1019543.
- [17] E. Kappenman and S. Luck, "The effects of electrode impedance on data quality and statistical significance in ERP recordings," *Psychophysiology*, vol. 47, no. 5, Sept. 2010, pp. 888-904, doi:10.1111/j.1469-8986.2010.01009.x.
- [18] I. Zepeda-Carapia, A. Márquez-Espinoza, and C. Alvarado-Serrano, "Measurement of Skin-Electrode Impedance for a 12-lead Electrocardiogram," Proc. Int. Conf. on Electrical and Electronic Eng., Sept. 2005, pp. 193-195, doi: 10.1109/ICEEE.2005.1529606.
- [19] Z. Li, Z. He, W. Wang, and C. Ren, "Measurement System for electrical impedance and EGG," Proc. 5th Int. Conf. on Information Techn. and Application on Biomedicine, May 2008, pp. 495-498, doi: 10.1109/ITAB.2008.4570598.
- [20] C. A. Grimbergen, A. C. MettingVanRijn, and A. Peper, "A method for the measurement of the properties of individual electrode-skin interfaces and the implications of the electrode properties for preamplifier design," Proc. 14th Annual Int. Conf. IEEE EMBS, vol. 6, Oct. 1992, pp. 2382-2383, doi: 10.1109/IEMBS.1992.5761414.
- [21] E. Spinelli, M. A. Mayosky, and R. Pallás-Areny, "A practical approach to electrode-skin impedance unbalance measurement," *IEEE Trans. on Biomedical Eng.*, vol. 53, no. 7, July 2006, pp. 1451-1453, doi: 10.1109/TBME.2006.875714.
- [22] R. Merletti, "The electrode-skin interface and optimal detection of bioelectric signals," *Physiol. Meas.*, vol. 31, no. 10, 2010, doi: doi:10.1088/0967-3334/31/10/E01.
- [23] C. Assambo, A. Baba, R. Dozio, and M. J. Burke, "Determination of the parameters of the electrode-skin impedance model for ECG measurements," Proc. of the 6th WSEAS Int. Conf. on Electronics, Hardware, Wireless and Optical Comm., Feb. 2007, pp. 90-95.
- [24] K. L. Kilgore, P. H. Peckham, M. W. Keith, and G. B. Thrope, "Electrode Characterization for functional application to

- upper extremity FNS," *IEEE Trans. Biomedical Eng.*, vol. 37, no. 1, Jan. 1990, pp.12-21, doi: 10.1109/10.43606.
- [25] T. Degen and H. Jäckel, "Continuous monitoring of electrode-skin impedance mismatch during bioelectric recordings," *IEEE Transactions on Biomedical Eng.*, vol. 55, no. 6, June 2008, pp. 1711-1715, doi: 10.1109/TBME.2008.919118.
- [26] S. Kim, R. F. Tazicioglu, T. Torfs, B. Dilpreet, P. Julien, and C. Van Hoof, "A 2.4 uA continuous-time electrode-skin impedance measurement circuit for motion artifact monitoring in ECG acquisition systems," *Proc. IEEE Symposium on VLSI Circuits*, June 2010, pp. 219-220, doi: 10.1109/VLSIC.2010.5560290.
- [27] A. Zambrano, F. Derogarian, R. Dias, M. J. Abreu, A. Catarino, A. M. Rocha, J. M. da Silva, J. C. Ferreira, V. G. Tavares, and M. V. Correia, "A wearable sensor network for human locomotion data capture," *Proc. 9th Int. Conf. on Wearable Micro and Nano Tech. for Personalized Health (pHealth)*, Porto, vol. 177, 2012, pp. 216-223.
- [28] H. J. Hermens, B. Freriks, R. Merletti, D. Stegeman, J. Blok, G. Rau, C. Disselhorst-Klug, and G. Hägg, "European Recommendations for Surface ElectroMyoGraphy", Enschede, the Netherlands: Roessingh Research and Development, 1999.
- [29] M. H. Zaki, S. Tahar, and G. Bois, "Formal verification of analog and mixed signal designs: a survey," *Microelectronics Journal*, vol. 39, Dec. 2008, pp. 1395-1404, doi:10.1016/j.mejo.2008.05.013.
- [30] M. Burns and G. W. Roberts, "An introduction to mixed-signal IC test and measurement", 2nd ed., New York, USA: Oxford University Press, 2011.
- [31] P. Tallgren, S. Vanhatalo, K. Kaila, and J. Voipio, "Evaluation of commercially available electrodes and gels for recording of slow EEG potentials," *Clinical Neurophysiology*, vol. 116, no. 4, Nov. 2005, pp. 799-806, doi:10.1016/j.clinph.2004.10.001.
- [32] Commission Electrotechnique Internationale, IEC 60601-1, 3rd ed., Geneva, Switzerland: IEC, 2005.
- [33] Association for the Advancement of Medical Instrumentation, Disposable ECG electrodes, American National Standards Institute, Inc., 2000.
- [34] S. Rogers, "Sensor noise fault detection," *Proc. of American Control Conference*, vol. 5, June 2003, pp. 4267-4268, doi: 10.1109/ACC.2003.1240506.
- [35] J. Feng, G. Qu, and M. Potkonjak, "Sensor calibration using nonparametric statistical characterization of error models," *Proc. of IEEE Sensors*, vol. 3, Oct. 2004, pp. 1456-1459, doi: 10.1109/ICSENS.2004.1426461.
- [36] T. Bourdenas and M. Sloman, "Towards self-healing in wireless sensor networks," *Proc. of Workshop on Wearable and Implantable Body Sensor Networks*, June 2009, pp. 15-20, doi: 10.1109/BSN.2009.14.
- [37] A. B. Sharma, L. Golubchik, and R. Govindan, "Sensor faults: detection methods and prevalence in real-world datasets," *ACM Transactions on Sensor networks*, vol. 6, no. 3, pp. 1-34, June 2010, doi: 10.1145/1754414.1754419.
- [38] E. U. Warriach, K. Tei, T. A. Nguyen, and M. Aiello, "Fault detection in wireless sensor networks: a hybrid approach," *Proc. of Int. Conf. on Information Processing in Sensor Net.*, pp- 87-88, April 2012, doi: 10.1145/2185677.2185690.
- [39] M. M. Puurtinen, S. M. Komulainen, P. K. Kauppinen, and J. A. Malmivuo, "Measurement of noise and impedance of dry and wet textile electrodes and textile electrode with hydrogel," *Proc. 28th IEEE Eng. in Medicine and Biology Society*, New York City, vol. 1, pp. 6012-6015, 2006.
- [40] J. C. Marquez, F. Seoane, E. Välimäki, and K. Lindcrantz, "Textile Electrodes in Electrical Bioimpedance Measurements - A Comparison with Conventional Ag/AgCl Electrodes," *Proc. IEEE Eng. in Medicine and Biology Society*, Minneapolis, Sept. 2009, pp. 4816-4819, doi: 10.1109/IEMBS.2009.5332631.
- [41] L. Beckmann, C. Neuhaus, G. Medrano, N. Jungbecker, M. Walter, T. Gries, and S. Leonhardt, "Characterization of textile electrodes and conductors using standardized measurement setups," *Physiological Measurements*, vol. 31, no. 2, Feb. 2010, pp. 233-247, doi: 10.1088/0967-3334/31/2/009.
- [42] J. G. Webster, *Medical Instrumentation: Application and Design*, 4th ed., Wiley, 2009.
- [43] M. L. Bushnell and V. D. Agrawal, *Essentials of electronic testing for digital, memory and mixed-signal VLSI circuits*, vol. 17, SCI-TECH Publishing Co., 2000.
- [44] J. Ziv and A. Lempel, "A universal algorithm for sequential data compression," *IEEE Trans. on Information Theory*, vol. 23, no. 3, May 1977, pp. 337-343, doi: 10.1109/TIT.1977.1055714.
- [45] A. J. Salazar, M. V. Correia, and J. M. Da Silva, "SCPS: Mixed-signal Test and Measurement Framework for Wearable Monitoring Systems," unpublished patent request submitted to Patent Office.
- [46] "I2C-bus specification and user manual, UM10204, Rev. 5," 2012.
- [47] V. R. Zschorlich, "Digital filtering of EMG-signals," *Electromyography and clinical neurophysiology*, vol. 29, no. 2, pp. 81-86, 1989.
- [48] B. Gerdle, S. Karlsson, S. Day, and M. Djupsjöbacka, "Acquisition, Processing and Analysis of the Surface Electromyogram," in *Modern Techniques in Neuroscience*, Berlin, Germany, Springer, 1999, pp. 705-755.